

NANO EXPRESS

Open Access

Mechanical characterization of nanoindented graphene via molecular dynamics simulations

Te-Hua Fang^{1*}, Tong Hong Wang², Jhih-Chin Yang³ and Yu-Jen Hsiao⁴

Abstract

The mechanical behavior of graphene under various indentation depths, velocities, and temperatures is studied using molecular dynamics analysis. The results show that the load, elastic and plastic energies, and relaxation force increased with increasing indentation depth and velocity. Nanoindentation induced pile ups and corrugations of the graphene. Resistance to deformation decreased at higher temperature. Strong adhesion caused topological defects and vacancies during the unloading process.

Keywords: molecular dynamics, nanoindentation, graphene, mechanical properties

Introduction

Graphene has received a lot of attention due to its good mechanical and electromagnetic properties [1-3], including a zero electron bandgap, a high electron emission rate, and elastic scattering [4-6]. Atomic-scale graphene can be fabricated using micro-mechanical chop crack [7], thermal expansion [8], and extension growth [9] techniques. Studies [10-13] have found that the band-field effect of a 10-nm-thick graphene sheet is similar to that of a small (less than 1.2 nm in diameter) nanographite particle.

Novoselov and Geim [7] used graphene to fabricate a small crystal tube. Monolayer graphene is considered a suitable material for investigating two-dimensional quantization phenomena, such as temperature-trigger plasma [14], quantization absorption spectrum [15], and the fractional quantum Hall effect [16]. In addition, the hexagonal symmetric structure of graphene makes it a candidate material for nano devices.

Many studies [17-25] have focused on the chemical functionalization of graphene, especially on the effect of absorbed atoms on the electronic and chemical properties of graphene. However, the mechanical properties of graphene under indentation, which are important for developing sensors, resonators, and impermeable membranes, have yet to be investigated.

In this study, the effects of nanoindentation depth and velocity on the mechanical properties and contact behavior of graphene at various temperatures are investigated using molecular dynamics (MD) simulations. Adhesion, relaxation, defects, and deformation are discussed.

Methodology

Figure 1 shows the MD model of a freestanding honeycomb graphene sheet and a diamond indenter tip. The graphene substrate consists of 10,032 carbon atoms over an area of 15.874×15.933 nm. In the model, three layers of carbon atoms are fixed using a bridge-type support and six carbon lateral layers of thermostat atoms are set as thermal layers. The other carbon atoms are Newtonian atoms. The hemispherical diamond tip has 344 carbon atoms and is treated as a rigid body. The diamond indenter is 1 nm above the graphene surface; it approaches the graphene surface at a constant velocity.

The Lennard-Jones potential function is employed to describe the interaction between the diamond tip and the graphene atoms. The Tersoff empirical potential energy function [10] is generally used to simulate the interaction between graphene carbon atoms.

Results and discussion

Figure 2 shows snapshots of graphene being indented by the hemispherical diamond tip at a velocity of 25 m/s, a hold time of 15 ps, and a temperature of 300 K. Thermal equilibrium was achieved before the indentation to

* Correspondence: fang.tehua@msa.hinet.net

¹Department of Mechanical Engineering, National Kaohsiung University of Applied Sciences, 415 Chien Kung Rd., Kaohsiung 807, Taiwan
Full list of author information is available at the end of the article

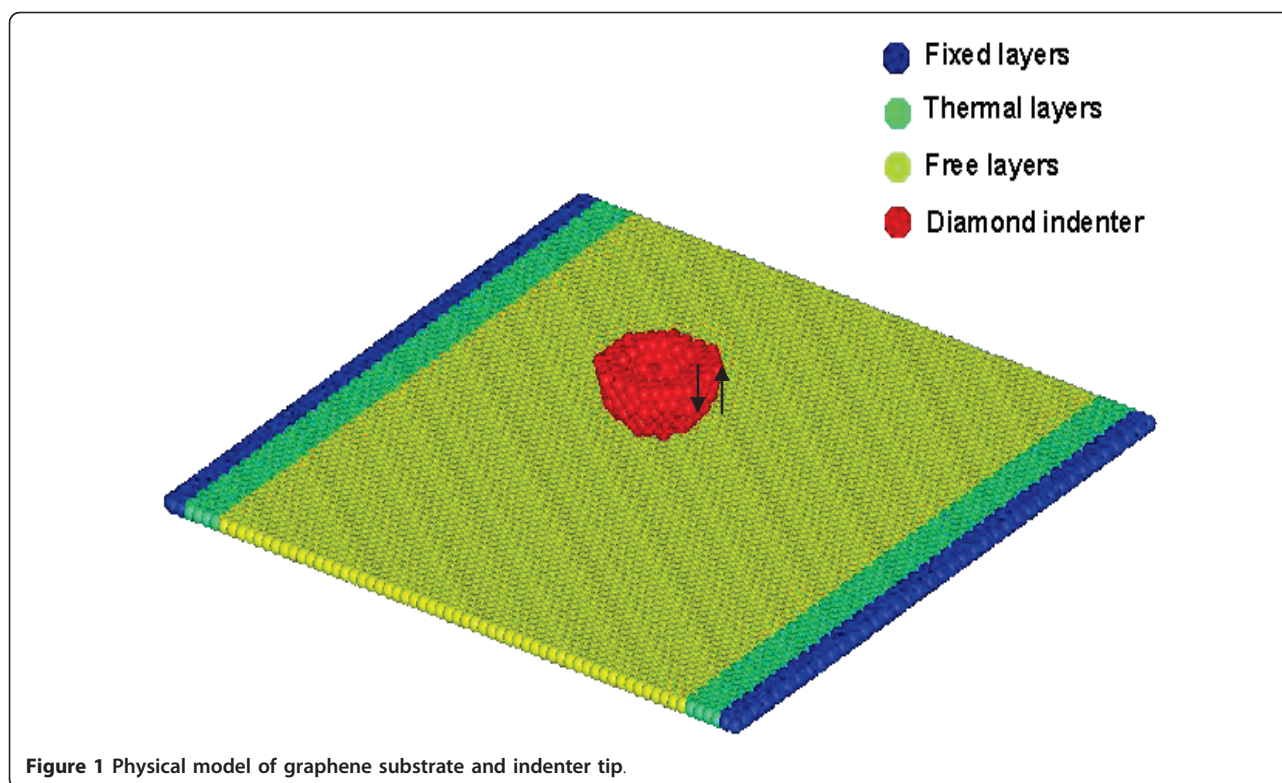


Figure 1 Physical model of graphene substrate and indenter tip.

have the atoms in a stable state. Figure 2a shows the initial contact of indentation at 33 ps. During indentation, the potential energy of the tip affects the surface atoms, especially those beneath the tip. Thus, some of the atoms jumped up and made contact with the tip, which is known as the jump-to-contact phenomenon.

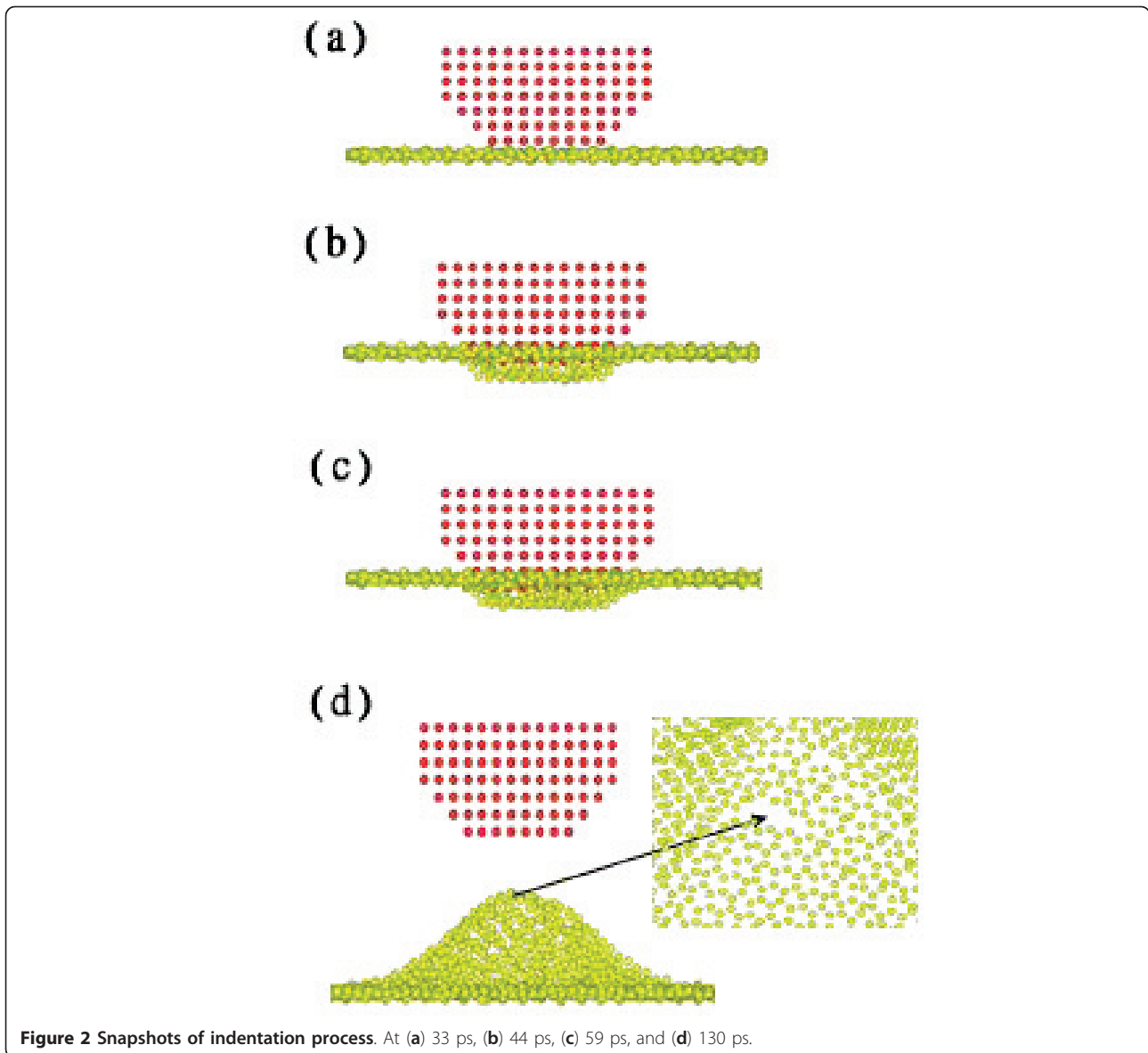
The tip then indented the graphene. The absorptive force gradually turns into a repulsive force. As the indentation depth increased, the stress wave spread out farther from the center, inducing ripples and corrugations. Figure 2b shows the tip at its maximum indentation depth. During the subsequent packing stage, the substrate releases the indentation-induced energy, as shown in Figure 2c. Finally, the tip moves up at a constant velocity (the same as that used for the indentation). Some substrate atoms beneath the tip move up during the unloading process to create a peak, as shown in Figure 2d.

The effect of indentation depth was examined. With all other conditions fixed, indentation depths of 0, 0.2, 0.4, and 0.6 nm were investigated. Figure 3 shows the force versus time curves for various indentation depths. The average maximum forces at indentation depths of 0, 0.2, 0.4, and 0.6 nm are 139.43, 195.47, 240.42, and 260.08 nN, respectively, indicating that the load increased with indentation depth. This is due to the number of atoms in contact with the tip increasing with indentation depth. Figure 4 shows the elastic energy and

plastic energy versus displacement curves. The elastic and plastic energies both increase with increasing displacement. The average relaxation forces are 123.71, 141.10, 156.00, and 161.21 nN for indentation depths of 0, 0.2, 0.4, and 0.6 nm, respectively. The central heights of the residual ripple after unloading are 0.998, 1.104, 1.253, and 1.3224 nm for indentation depths of 0, 0.2, 0.4, and 0.6 nm, respectively.

Figure 5 shows the topographies obtained for various indentation depths. The peak is larger for a deeper indentation due to more atoms adhering to the tip. Pile ups and corrugations of the graphene occurred beneath the indenter tip. The strong adhesion led to topological defects and vacancies. Stone-Wales defects usually play an important role in the corrugation region with 5-7-7-5 ring defects [26]. We also found double vacancy (C_2) defects, which are composed of one octagonal ring and two pentagonal rings, during the adhesion pulling process. Double vacancies are referred to as 5-8-5 defects [27]. Our simulation results agree with those reported by Kudin et al. [28], who investigated the Raman spectra of graphite oxide and functionalized graphene sheets with Stone-Wales defects and C_2 defects [28].

Figure 6 shows the load versus time curves for temperatures of 0, 200, 300, and 400 K, respectively, with a velocity of 25 m/s and a packing time of 15 ps. At lower temperature, a higher force was required to achieve a given indentation depth due to the higher hardness of



the material. The average maximum forces at sample temperatures of 0, 200, 300, and 400 K are 221.57, 191.24, 181.59, and 172.10 nN, respectively. Temperature control is thus necessary for a stable mechanical response. The average contact stiffnesses of the graphene at temperatures of 0, 200, 300, and 400 K are 58.7, 58.1, 49.48, and 36.6 N/m, respectively.

Figure 7 shows the elastic energy and plastic energy versus temperature curves. Both energies decrease with increasing temperature due to the increasing distance between atoms. Reduced relaxation forces were calculated to be 176.25, 167.38, 159.705, and 152.14 nN for 0, 200, 300, and 400 K, respectively. However, the topographies obtained at the various temperatures, as shown in Figure 8, only slightly changed. The central heights of the

residual ripple after unloading are 0.946, 1.026, 1.041, and 1.047 nm for 0, 200, 300, and 400 K, respectively.

Indentation velocities of 25, 50, 75, and 100 m/s were tested by fixing the temperature at 300 K and the packing time at 15 ps. Figure 9 shows the load versus time curves for various indentation velocities. The load increases with increasing indentation velocity. This is due to the atoms having enough time to release and transfer internal residual stress at slower indentation velocities. The central heights of the residual ripple after unloading are 1.041, 0.907, 0.698, and 0.689 nm for indentation velocities of 25, 50, 75, and 100 m/s, respectively.

Figure 10 shows the elastic energy and plastic energy versus indentation velocity curves. Both energies

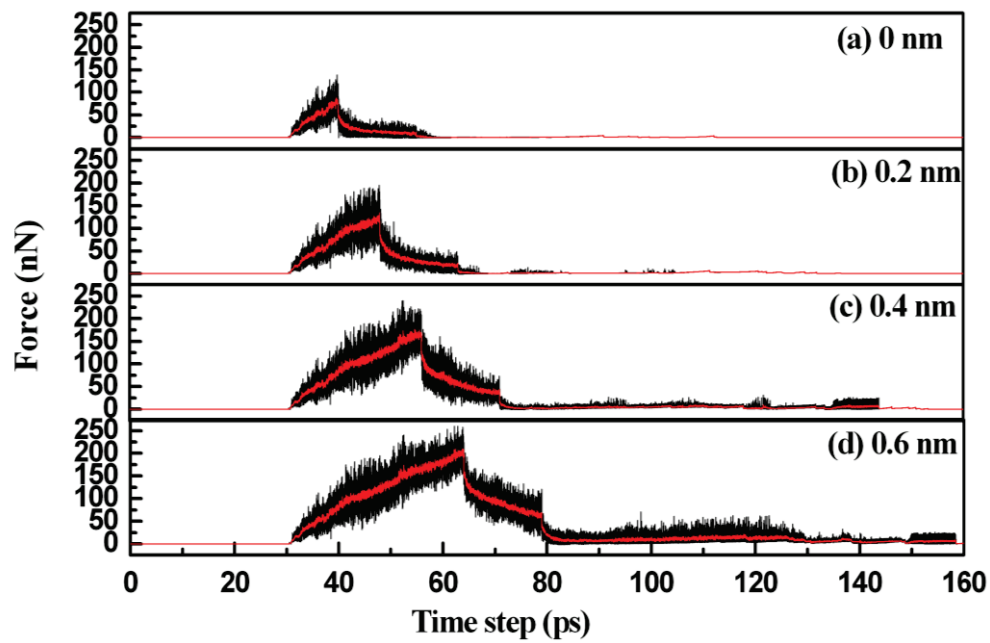


Figure 3 Load versus time for various indentation depths.

increase with increasing velocity. Relaxation forces of 159.05, 222.93, 280.94, and 314.56 nN were obtained for indentation velocities of 25, 50, 75, and 100 m/s, respectively. Figure 11 shows the topographies obtained for

various velocities. A slower indentation allows more atoms to adhere on the tip, and thus a larger area of the substrate is pulled up during tip unloading, forming a higher peak.

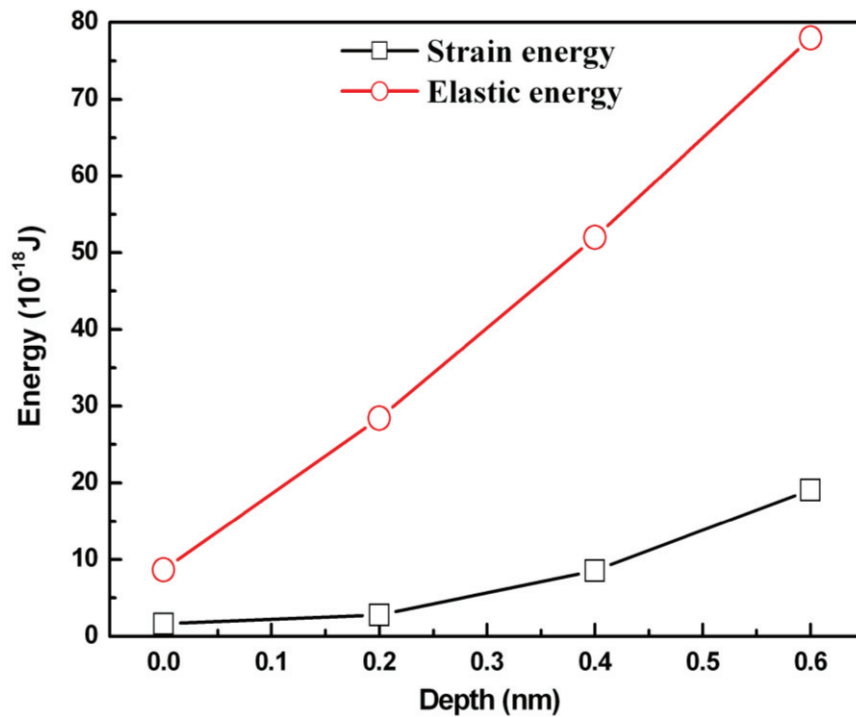


Figure 4 Elastic energy and plastic energy versus indentation depth.

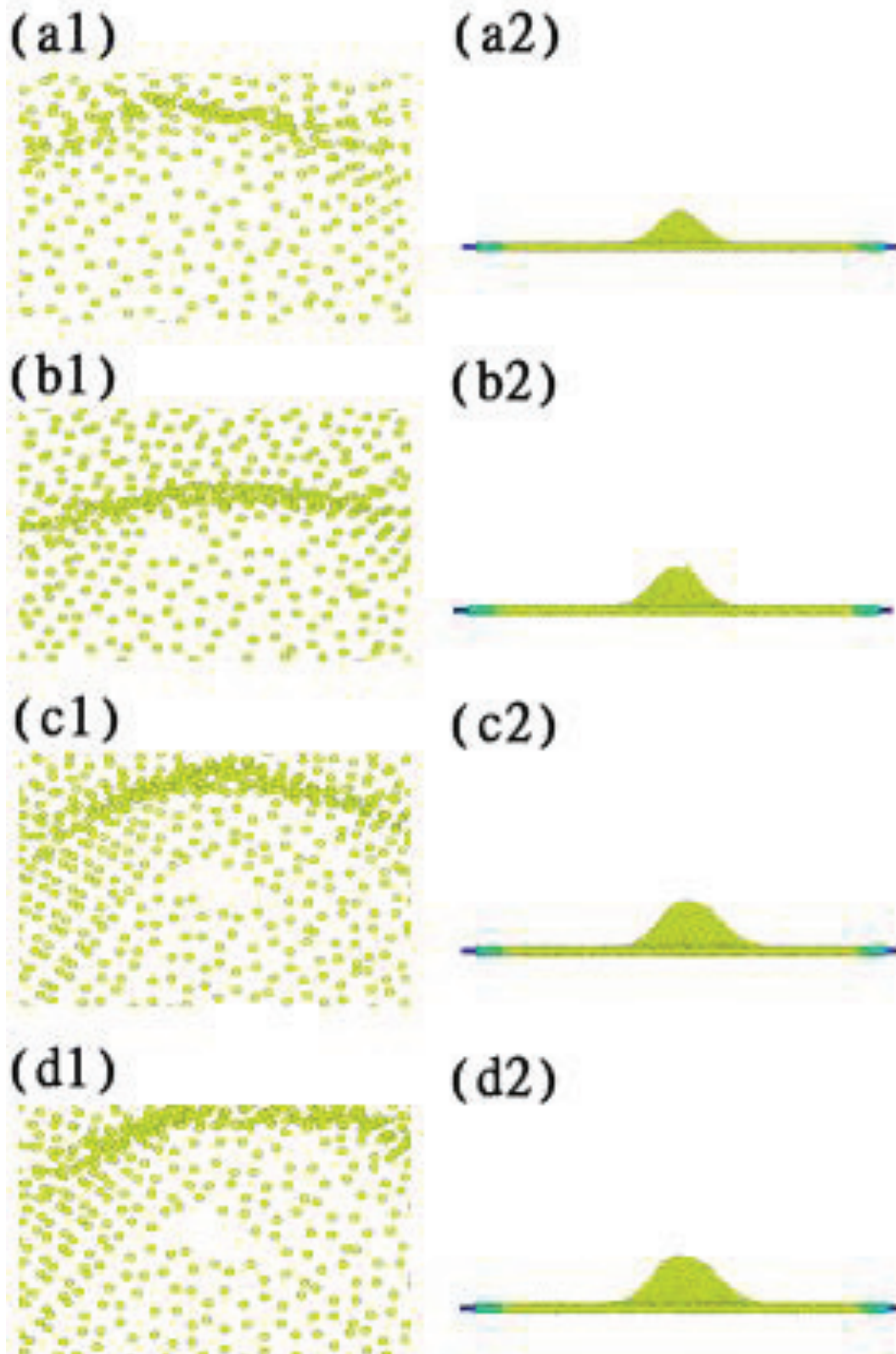


Figure 5 Topographies for indentations. Indentations of (a1, a2) 0 nm, (b1, b2) 0.2 nm, (c1, c2) 0.4 nm, and (d1, d2) 0.6 nm.

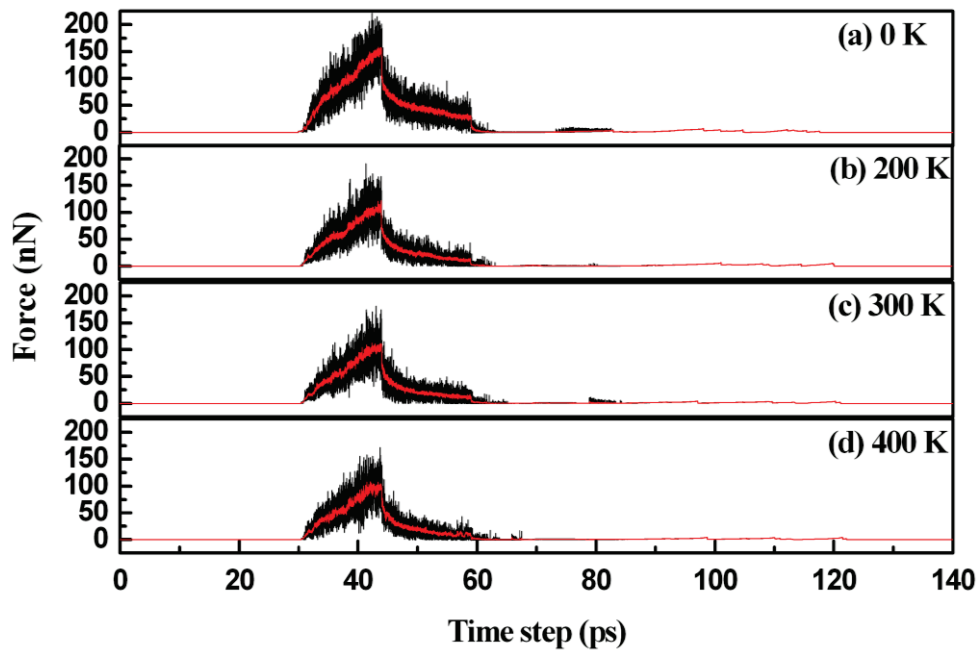


Figure 6 Load versus time for various temperatures.

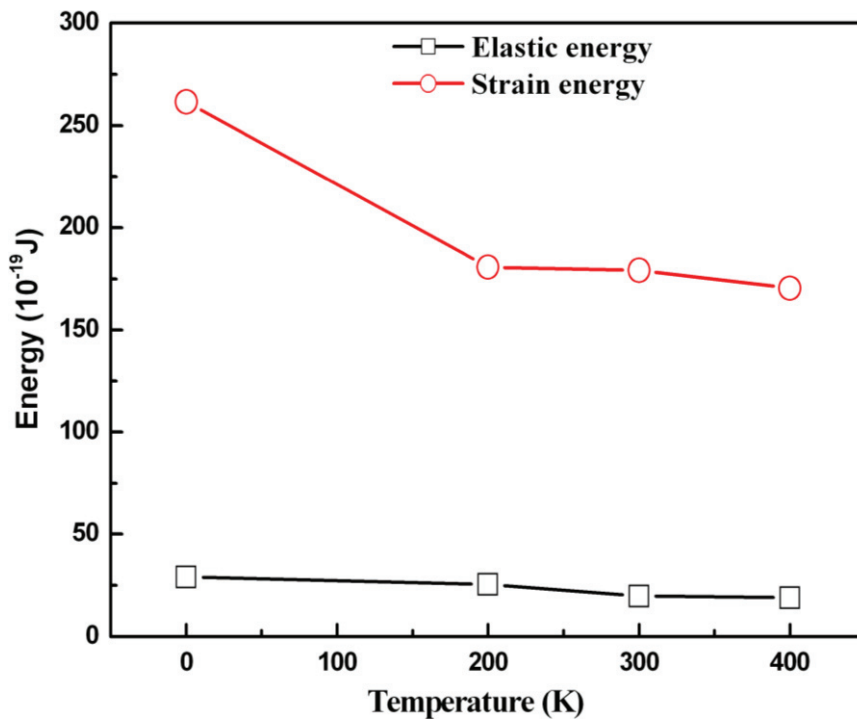


Figure 7 Elastic energy and plastic energy versus temperature.

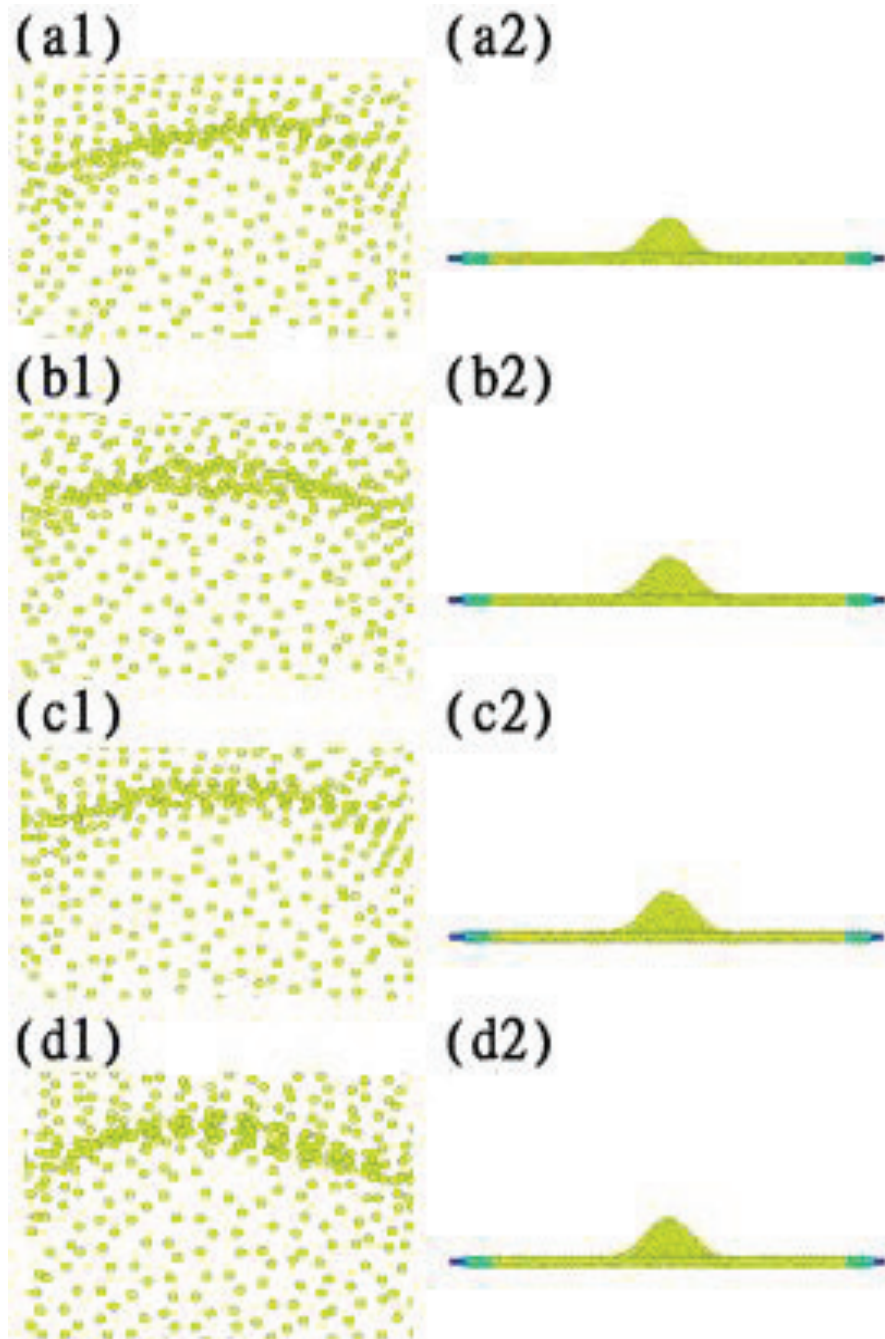


Figure 8 Topographies for temperatures. Temperatures at (a1, a2) 0 K, (b1, b2) 200 K, (c1, c2) 300 K, and (d1, d2) 400 K.

Conclusion

The indentation behavior of graphene was studied using molecular dynamics simulations. The following conclusions were obtained:

1. The affected area, load, elastic and plastic energies, and relaxation force increased with increasing indentation depth.

2. Nanoindentation-induced pile ups and corrugations of graphene were observed. Strong adhesion causes topological defects and vacancies.

3. The average contact stiffnesses of the graphene at temperatures of 0, 200, 300, and 400 K are 58.7, 58.1, 49.48, and 36.6 N/m, respectively.

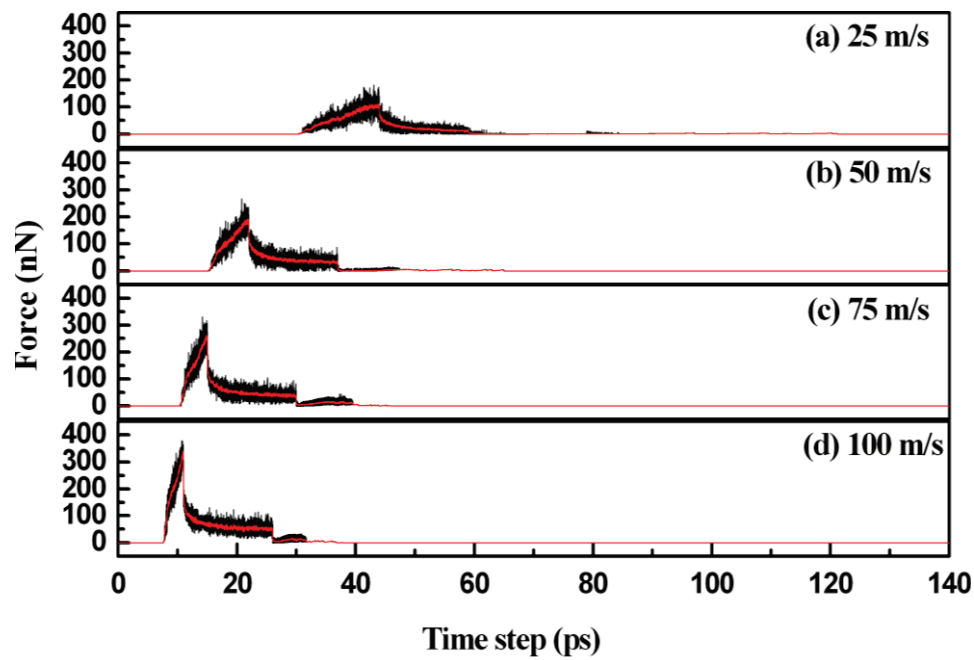


Figure 9 Load versus time for various velocities.

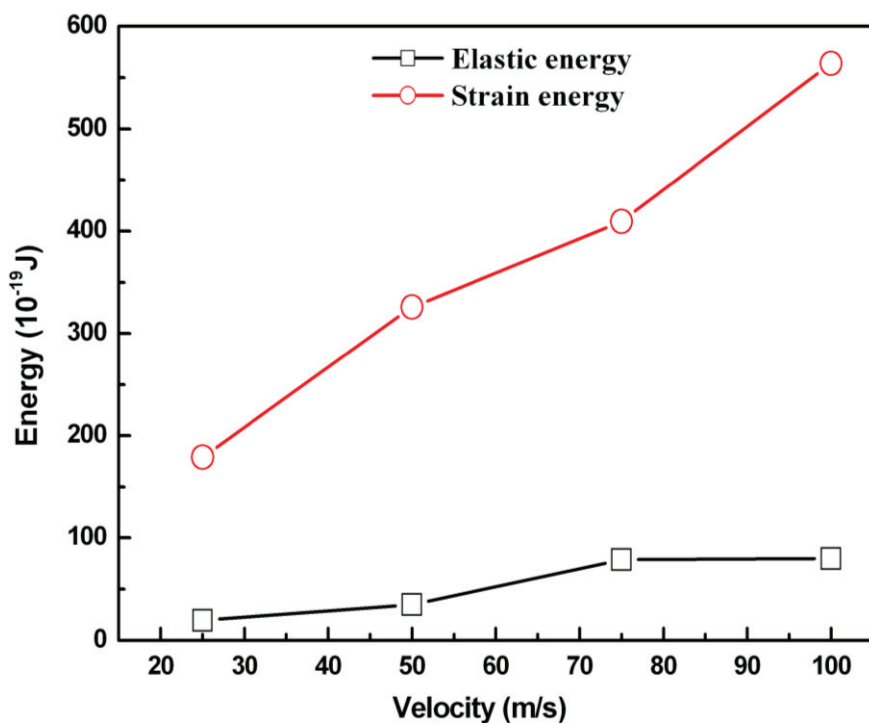


Figure 10 Elastic energy and plastic energy versus velocity.

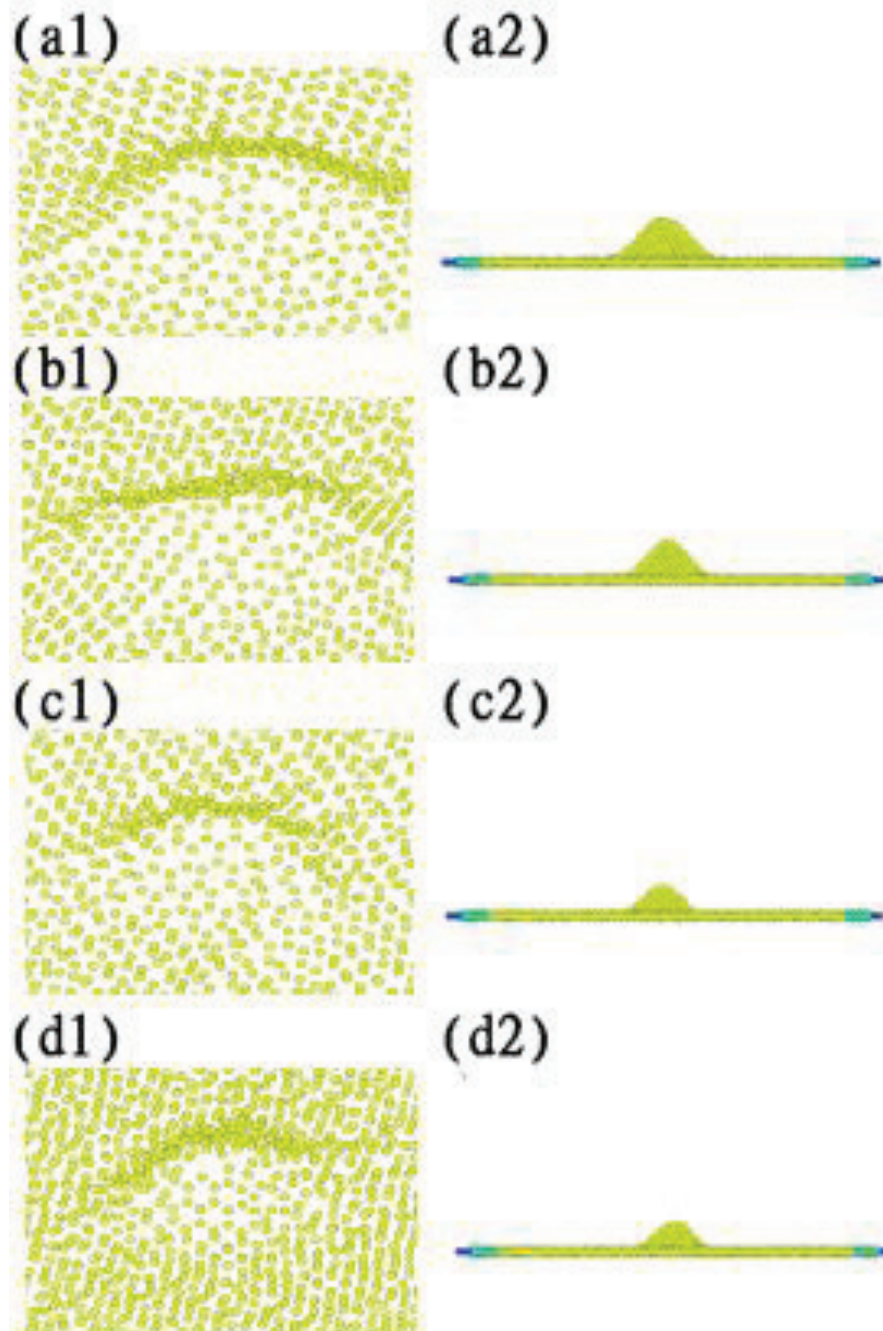


Figure 11 Topographies for velocities. Velocities of (a1, a2) 25 m/s, (b1, b2) 50 m/s, (c1, c2) 75 m/s, and (d1, d2) 100 m/s.

4. At higher temperature, the kinetic energy among atoms increases, which weakens covalent bonds and thus decreases resistance to deformation. The load, elastic and plastic energies, and relaxation force decrease with increasing temperature.

5. With a fast indentation, the graphene has insufficient time to respond, which leads to a high load, elastic and plastic energies, and relaxation force.

Acknowledgements

The authors would like to thank the National Science Council of Taiwan for financially supporting this research under grant NSC 96-2628-E-151-004-MY3.

Author details

¹Department of Mechanical Engineering, National Kaohsiung University of Applied Sciences, 415 Chien Kung Rd., Kaohsiung 807, Taiwan ²Central Product Solutions, Advanced Semiconductor Engineering, Inc., Kaohsiung 811, Taiwan ³Institute of Mechanical and Electromechanical Engineering,

National Formosa University, Yunlin 632, Taiwan ⁴National Nano Device Laboratories, Tainan 741, Taiwan

Authors' contributions

The work presented here was carried out in collaboration between all authors. THF, THW and JCY defined the research theme. THF and JCY designed methods and analyzed the data, interpreted the results and wrote the paper. YJH co-worked on associated data collection, their interpretation, and presentation. All authors have contributed to, seen and approved the final manuscript.

Competing interests

The authors declare that they have no competing interests.

Received: 16 January 2011 Accepted: 3 August 2011
Published: 3 August 2011

References

1. Lijima S: Helical microtubules of graphitic carbon. *Nature* 1991, **354**:56.
2. Kong J, Chapline MG, Dai H: Functionalized carbon nanotubes for molecular hydrogen sensors. *Adv Mater* 2001, **13**:1384.
3. Wu J, Pisula W, Müllen K: Graphenes as potential material for electronics. *Chem Rev* 2007, **107**:718.
4. Novoselov KS, Geim AK, Morozov SV, Jiang D, Katsnelson MI, Grigorieva IV, Dubonos SV, Firsov AA: Two-dimensional gas of massless Dirac fermions in graphene. *Nature* 2005, **438**:197.
5. Zhang Y, Tan YW, Stormer HL, Kim P: Experimental observation of the quantum Hall effect and Berry's phase in graphene. *Nature* 2005, **438**:201.
6. Novoselov KS, Jiang D, Schedin F, Booth TJ, Khotkevich VV, Morozov SV, Geim AK: Two-dimensional atomic crystals. *Proc Natl Acad Sci USA* 2005, **102**:10451.
7. Novoselov KS, Geim AK, Morozov SV, Jiang D, Zhang Y, Dubonos SV, Firsov AA: Electric field effect in atomically thin carbon films. *Science* 2004, **306**:666.
8. Schnoepf HC, Li JL, McAllister MJ, Sai M, Herrera-Alonso H, Adamson DH, Prud'Homme RK, Car R, Saville DA, Aksay IA: Functionalized single graphene sheets derived from splitting graphite oxide. *J Phys Chem B* 2007, **110**:8535.
9. Berger C, Song Z, Li T, Li X, Ogbazghi AY, Feng R, Dai Z, Marchenkov AN, Conrad EH, First TN, de Heer WA: Ultrathin epitaxial graphite: 2D electron gas properties and a route toward graphene-based nanoelectronics. *J Phys Chem B* 2004, **108**:19912.
10. Tersoff J: Empirical interatomic potential for carbon, with applications to amorphous carbon. *Phys Rev Lett* 1988, **61**:2879.
11. Hölscher H, Ebeling D, Schwarz UD: Friction at atomic-scale surface steps: experiment and theory. *Phys Rev Lett* 2008, **101**:246105.
12. Wang X, Ouyang Y, Li X, Wang H, Guo J, Dai H: Room-temperature all-semiconducting sub-10-nm graphene nanoribbon field-effect transistors. *Phys Rev Lett* 2008, **100**:206803.
13. Ponomarenko LA, Schedin F, Katsnelson MI, Yang R, Hill EW, Novoselov KS, Geim AK: Chaotic dirac billiard in graphene quantum dots. *Science* 2008, **320**:356.
14. Shyu FL, Lin MF: Plasmons and optical properties of semimetal graphite. *J Phys Soc Jpn* 2000, **69**:3781.
15. Sadowski ML, Martinez G, Potemski M, Berger C, de Heer WA: Landau level spectroscopy of ultrathin graphite layers. *Phys Rev Lett* 2006, **97**:266405.
16. Zang Y, Tan YW, Stormer HL, Kim P: Experimental observation of the quantum Hall effect and Berry's phase in graphene. *Nature* 2005, **438**:201.
17. Boukhvalov DW, Katsnelson MI: Chemical functionalization of grapheme. *J Phys Condens Matter* 2009, **21**:344250.
18. Boukhvalov DW, Katsnelson MI: Chemical functionalization of graphene with defects. *Nano Lett* 2008, **8**:4373.
19. Ou Yang F, Huang B, Li Z, Xiao J, Wang H, Xu H: Chemical functionalization of graphene nanoribbons by carboxyl groups on Stone-Wales defects. *J Phys Chem C* 2008, **112**:12003.
20. Kudin KN: Zigzag graphene nanoribbons with saturated edges. *ACS Nano* 2008, **2**:516.
21. Li Y, Ding F, Yakobson BI: Hydrogen storage by spillover on graphene as a phase nucleation process. *Phys Rev B* 2008, **78**:041402.
22. Roman T, Dino WA, Nakanishi H, Kasai H, Sugimoto T, Tange K: Hydrogen pairing on graphene. *Carbon* 2007, **45**:218.
23. Ramanathan T, Abdala AA, Stankovich S, Dikin DA, Herrera-Alonso M, Piner RD, Adamson DH, Schniepp HC, Chen X, Ruoff RS, Nguyen ST, Aksay IA, Prud'homme RK, Brinson LC: Functionalized graphene sheets for polymer nanocomposites. *Nature Nanotechnology* 2008, **3**:327.
24. Duplock EJ, Scheffler M, Lindan PJD: Hallmark of perfect graphene. *Phys Rev Lett* 2004, **92**:225502.
25. Boukhvalov DW, Katsnelson MI, Lichtenstein AI: Hydrogen on graphene: electronic structure, total energy, structural distortions and magnetism from first-principles calculations. *Phys Rev B* 2008, **77**:035427.
26. We CD, Fang TH, Chan CY: A molecular dynamics simulation of the mechanical characteristics of a C₆₀-filled carbon nanotube under nanoindentation using various carbon nanotube tips. *Carbon* 2011, **49**:2053.
27. Lee GD, Wang CZ, Yoon E, Hwang NM, Kim DY, Ho KM: Diffusion, coalescence, and reconstruction of vacancy defects in graphene layers. *Phys Rev Lett* 2005, **95**:205501.
28. Kudin KN, Ozbas B, Schniepp HC, Prud'homme RK, Aksay IA, Car R: Raman spectra of graphite oxide and functionalized graphene sheets. *Nano Lett* 2008, **8**:36.

doi:10.1186/1556-276X-6-481

Cite this article as: Fang et al.: Mechanical characterization of nanoindented graphene via molecular dynamics simulations. *Nanoscale Research Letters* 2011 **6**:481.

Submit your manuscript to a SpringerOpen® journal and benefit from:

- Convenient online submission
- Rigorous peer review
- Immediate publication on acceptance
- Open access: articles freely available online
- High visibility within the field
- Retaining the copyright to your article

Submit your next manuscript at ► springeropen.com